Coupling of light from microdisk lasers into plasmonic nano-antennas

Haroldo T. Hattori[1,*], Ziyuan Li[1], Danyu Liu[2], Ivan D. Rukhlenko[3], and Malin Premaratne[3]

[1]*School of Engineering and Information Technology, University of New South Wales, Australian Defence Force Academy, Canberra, ACT 2600, Australia*

[2] *Department of Electronic Materials Engineering, Research School of Physics and Engineering, Australian National University, Canberra ACT 0200, Australia.*

[3] *Advanced Computing and Simulation Laboratory (AXL), Department of Electrical and Computer Systems Engineering, Monash University, Clayton, VIC 3800, Australia*

h.hattori@adfa.edu.au

Abstract: An optical dipole nano-antenna can be constructed by placing a sub-wavelength dielectric (e.g., air) gap between two metallic regions. For typical applications using light in the infrared region, the gap width is generally in the range between 50 and 100 nm. Owing to the close proximity of the electrodes, these antennas can generate very intense electric fields that can be used to excite nonlinear effects. For example, it is possible to trigger surface Raman scattering on molecules placed in the vicinity of the nano-antenna, allowing the fabrication of biological sensors and imaging systems in the nanometric scale. However, since nano-antennas are passive devices, they need to receive light from external sources that are generally much larger than the antennas. In this article, we numerically study the coupling of light from microdisk lasers into plasmonic nano-antennas. We show that, by using micro-cavities, we can further enhance the electric fields inside the nano-antennas.

OCIS codes: (130.0130) Integrated Optics; (140.5960) Semiconductor lasers; (240.6680) Surface plasmons.

References and links

1. S. A. Maier, *Plasmonics: Fundamentals and Applications* (Springer, New York, 2007).
2. C. Genet, and T. W. Ebbesen, "Light in tiny holes," Nature **445**(7123), 39–46 (2007).
3. A. Boltasseva, S. I. Bozhevolnyi, T. Søndergaard, T. Nikolajsen, and K. Leosson, "Compact Z-add-drop wavelength filters for long-range surface plasmon polaritons," Opt. Express **13**(11), 4237–4243 (2005), http://www.opticsexpress.org/abstract.cfm?URI=oe-13-11-4237.
4. S. A. Maier, P. G. Kik, H. A. Atwater, S. Meltzer, E. Harel, B. E. Koel, and A. A. G. Requicha, "Local detection of electromagnetic energy transport below the diffraction limit in metal nanoparticle plasmon waveguides," Nat. Mater. **2**(4), 229–232 (2003).
5. J. C. Weeber, M. U. Gonzalez, A. L. Baudrion, and A. Dereux, "Surface Plasmon routing along right angle bent metal stripes," Appl. Phys. Lett. **87**(22), 221101 (2005).
6. A. Minovich, H. T. Hattori, I. McKerracher, H. H. Tan, D. N. Neshev, C. Jagadish, and Y. S. Kivshar, "Enhanced transmission of light through periodic and chirped lattices of nanoholes," Opt. Commun. **282**(10), 2023–2027 (2009).
7. V. A. Poldoskiy, A. K. Sarychev, and V. M. Shalaev, "Plasmon modes in metal nanowires and left-handed materials," J. Nonlinear Opt. Phys. Mater. **11**(1), 65–74 (2002).
8. H. Fischer, and O. J. F. Martin, "Engineering the optical response of plasmonic nanoantennas," Opt. Express **16**(12), 9144–9154 (2008), http://www.opticsinfobase.org/oe/abstract.cfm?URI=oe-16-12-9144.
9. N. Yu, E. Cubukcu, L. Diehl, D. Bour, S. Corzine, J. Zhu, G. Höfler, K. B. Crozier, and F. Capasso, "Bowtie plasmonic quantum cascade laser antenna," Opt. Express **15**(20), 13272–13281 (2007), http://www.opticsinfobase.org/oe/abstract.cfm?URI=oe-15-20-13272.
10. J. Li, A. Salandrino, and N. Engheta, "Shaping light beams in the nanometer scale: A Yagi-Uda nanoantenna in the optical domain," Phys. Rev. B **76**(24), 245403–245407 (2007).
11. M. L. Brongersma, "Engineering optical nanoantennas," Nat. Photonics **2**(5), 270–272 (2008).
12. J. Merlein, M. Kahl, A. Zuschlag, A. Sell, A. Halm, J. Boneberg, P. Leiderer, A. Leitenstorfer, and R. Bratschitsch, "Nanomechanical control of an optical nano-antenna," Nat. Photonics **2**(4), 230–233 (2008).

#118416 - $15.00 USD Received 12 Oct 2009; revised 23 Oct 2009; accepted 27 Oct 2009; published 30 Oct 2009

13. A. Alù, and N. Engheta, "Tuning the scattering response of optical nanoantennas with nanocircuit loads," Nat. Photonics **2**(5), 307–310 (2008).
14. N. Yu, R. Blanchard, J. Fan, Q. J. Wang, C. Pflügl, L. Diehl, T. Edamura, M. Yamanishi, H. Kan, and F. Capasso, "Quantum cascade lasers with integrated plasmonic antenna-array collimators," Opt. Express **16**(24), 19447–19461 (2008), http://www.opticsinfobase.org/oe/abstract.cfm?URI=oe-16-24-19447.
15. H. G. Park, J. K. Hwang, J. Huh, H. Y. Ryu, S. H. Kim, J. S. Kim, and Y. H. Lee, "Characteristics of modified single-defect two-dimensional photonic crystal lasers," IEEE J. Quantum Electron. **38**(10), 1353–1365 (2002).
16. N. Yokouchi, A. J. Danner, and K. D. Choquette, "Vertical-cavity surface-emitting laser operating with photonic crystal seven-point defect structure," Appl. Phys. Lett. **82**(21), 3608–3610 (2003).
17. H. T. Hattori, C. Seassal, X. Letartre, P. Rojo-Romeo, J. L. Leclercq, P. Viktorovitch, M. Zussy, L. di Cioccio, L. El Melhaoui, and J. M. Fedeli, "Coupling analysis of heterogeneous integrated InP based photonic crystal triangular lattice band-edge lasers and silicon waveguides," Opt. Express **13**(9), 3310–3322 (2005), http://www.opticsinfobase.org/oe/abstract.cfm?URI=oe-13-9-3310.
18. H. T. Hattori, V. M. Schneider, R. M. Cazo, and C. L. Barbosa, "Analysis of strategies to improve the directionality of square lattice band-edge photonic crystal structures," Appl. Opt. **44**(15), 3069–3076 (2005).
19. R. M. Cazo, C. L. Barbosa, H. T. Hattori, and V. M. Schneider, "Steady-state analysis of a directional square lattice band-edge photonic crystal laser," Microw. Opt. Technol. Lett. **46**(3), 210–214 (2005).
20. D. Ohnishi, T. Okano, M. Imada, and S. Noda, "Room temperature continuous wave operation of a surface-emitting two-dimensional photonic crystal diode laser," Opt. Express **12**(8), 1562–1568 (2004).
21. S. J. Choi, K. Djordjev, and P. D. Dapkus, "Microdisk lasers vertically coupled to output waveguides," IEEE Photon. Technol. Lett. **15**(10), 1330–1332 (2003).
22. S. V. Boriskina, T. M. Benson, P. D. Sewell, and A. I. Nosich, "Directional emission, increased free spectral range, and mode Q-factors in 2-D wavelength scale optical microcavity structures," IEEE J. Sel. Top. Quantum Electron. **12**, 1175–1182 (2006).
23. M. Fujita, R. Ushigone, and T. Baba, "Continuous wave lasing in GaInAsP injection laser with threshold current of 40 μA," Electron. Lett. **36**, 790–791 (2000).
24. H. T. Hattori, D. Liu, H. H. Tan, and C. Jagadish, "Large square resonator laser with quasi-single-mode operation," IEEE Photon. Lett. **21**(6), 359–361 (2009).
25. Fullwave 6.1 RSOFT design group, 2008, *http://www.rsoftdesign.com*
26. Y. Z. Huang, and Y. D. Yang, "Mode coupling and vertical radiation loss for whispering gallery modes in 3-D microcavities," IEEE/OSA, J. Lightwave Technol. **26**(11), 1411–1416 (2008).
27. H. T. Hattori, "Modal analysis of one-dimensional nonuniform arrays of square resonators," J. Opt. Soc. Am. B **25**(11), 1873–1881 (2008).

1. Introduction

Surface plasmon polaritons (plasmonic waves) are electromagnetic excitations propagating at the interface between a dielectric and a conductor, evanescently confined in the normal direction [1]. A few years ago, it was shown that the excitation of plasmonic waves could lead to the transmission of light at sub-wavelength range [2], creating the possibility of developing tiny optical components with dimensions smaller than the wavelength of light [3–7]. Another important aspect of the excitation of plasmonic waves is the strong enhancement of the incident electric fields near the surface of the metallic regions by several orders of magnitude [8,9]. These regions of intense electric fields ("hot" regions) can excite localized nonlinear effects such as the surface enhanced Raman scattering. The excitation of high intense electric fields at sub-wavelength regions can be achieved by using plasmonic devices called nano-antennas. One simple example of nano-antenna is a dipole antenna, where a sub-wavelength air gap between two metallic regions can enhance the electric field more than 100 times [9].

The properties of nano-antennas have been extensively discussed (see, for example [9–13],). Besides applications in biological sensing and imaging, these nano-antennas can be used to manipulate nano-particles that are attracted by the high intense fields generated in the gap between the metallic regions. Recently, nano-antennas have also been used to collimate the far-field emission from semiconductor lasers [14].

These exciting applications have fostered the research on nano-antennas by several research groups worldwide. However, light has been coupled from large area semiconductor lasers (e.g. Fabry-Perot lasers with transversal areas of several micrometers) into nano-antennas with nanometric gaps. This way of coupling light into the nano-antenna is not efficient since most of the emitted light is not directly coupled into the nano-antenna but lost elsewhere. Moreover, more compact laser sources such as photonic crystal [15–20] and polygonal lasers [21–24] could be used to excite these tiny antennas. In this article, we examine the coupling of light from a microdisk laser into nano-antennas with dimensions

#118416 - $15.00 USD Received 12 Oct 2009; revised 23 Oct 2009; accepted 27 Oct 2009; published 30 Oct 2009

between 50 and 100 nm: different coupling schemes are analyzed and their performances are assessed. We show that coupling of light into dipole nano-antennas can be tricky, since the metallic surfaces act as reflectors of the incident wave, leading to additional resonant peaks in the microdisk structure. Although the introduction of micro-cavities to the nano-antennas create additional resonant peaks in the microdisk resonator, the addition of these cavities can increase the electric field inside the nano-antenna and, at the same time, improve the coupling efficiency into the device.

2. Stand-alone microdisk structure and direct coupling into the nano-antenna

A schematic diagram of an epitaxially layered structure that could be used to fabricate these devices is shown in Fig. 1(a). The core layer consists of GaAs with three $In_{0.5}Ga_{0.5}As$ quantum dot layers, whose vertical confinement is provided by a low refractive index air top layer (total internal reflection) and a bottom Bragg stack layer (working in its bandgap region). The Bragg stack layer consists of 25 pairs of alternating quarter wavelength AlAs and GaAs layers, providing a reflectivity above 99%. The quantum dots have diameters ranging from 20 to 30 nm and heights between 3 to 5 nm, with an average quantum dot concentration of $4x10^{10}$ cm^{-2}. The separation between different quantum dot layers is about 30 nm. These quantum dots can be grown by a Metal Organic Chemical Vapor Deposition (MOCVD) system by using a Stranski-Krastanov method. These quantum dots have a gain peak at 1160 nm with a gain bandwidth of about 100 nm.

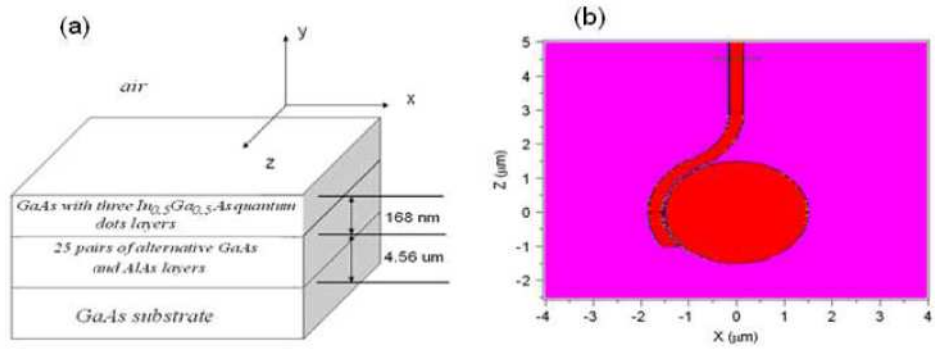

Fig. 1. (a) Schematic of the epitaxially layered structure and (b) Microdisk laser coupled to a single-mode waveguide.

In order to analyze different optical devices, commercial three-dimensional finite difference time domain (FDTD) software [25] is employed. The mode is assumed to be TE, with main component of the magnetic field in the y-direction (H_y), perpendicular to the plane of the device [see Fig. 1(a)]. A light source is placed at the edge of the microdisk laser and is assumed to be Gaussian, with a spot-size diameter of 300 nm. The computation region is terminated by perfectly matched absorbing layers. The grid size specified in the calculations is uniform along the x and z directions, (with grid sizes of 30 nm) and the time step $\Delta t=6.7x10^{-18}$ s. No material gain is added to these simulations because we are trying to assess coupling efficiencies.

We first consider a scenario in which a stand-alone microdisk is coupling light into a single-mode waveguide as shown in Fig. 1(b). The single-mode waveguide has a width of 300 nm and supports a single mode at the wavelength of 1160 nm. The radius of the microdisk is 1.5 μm and the gap between the microdisk laser and the waveguide is 100 nm. The field spectrum (H_y) for this microdisk laser is shown in Fig. 2(a) in the range between 1100 and 1200 nm. The main resonant peak appears at the free-space wavelength λ = 1166 nm with a quality factor (Q) of 16000. This mode corresponds to $TE_{17,1}$ using the same convention as in [26] (the first index corresponds to the azimuthal mode number and the second index is the radial mode number). Another resonant peak appears close to the edge of the gain bandwidth (λ = 1116 nm), with Q = 8000. A power budget analysis indicates that about 38% of the input

#118416 - $15.00 USD Received 12 Oct 2009; revised 23 Oct 2009; accepted 27 Oct 2009; published 30 Oct 2009

power is coupled into the waveguide. The magnetic field distribution (H_y) at this wavelength is shown in Fig. 2(b). The resonant mode frequencies of the microdisk are determined by solving the following eigenmode equation [26]:

$$J_m(n_{eff}kR)H_m^{'(2)}(KR) = \eta J_m^{'}(n_{eff}kR)H_m^{(2)}(KR) \quad (1)$$

where J_m and $H^{(2)}{}_m$ are the Bessel and second-kind Hankel functions of order m, k is the free-space wave number, R is the radius of the microdisk, n_{eff} is the effective refractive index of the TE mode, and η is $1/n_{eff}$ for TE modes.

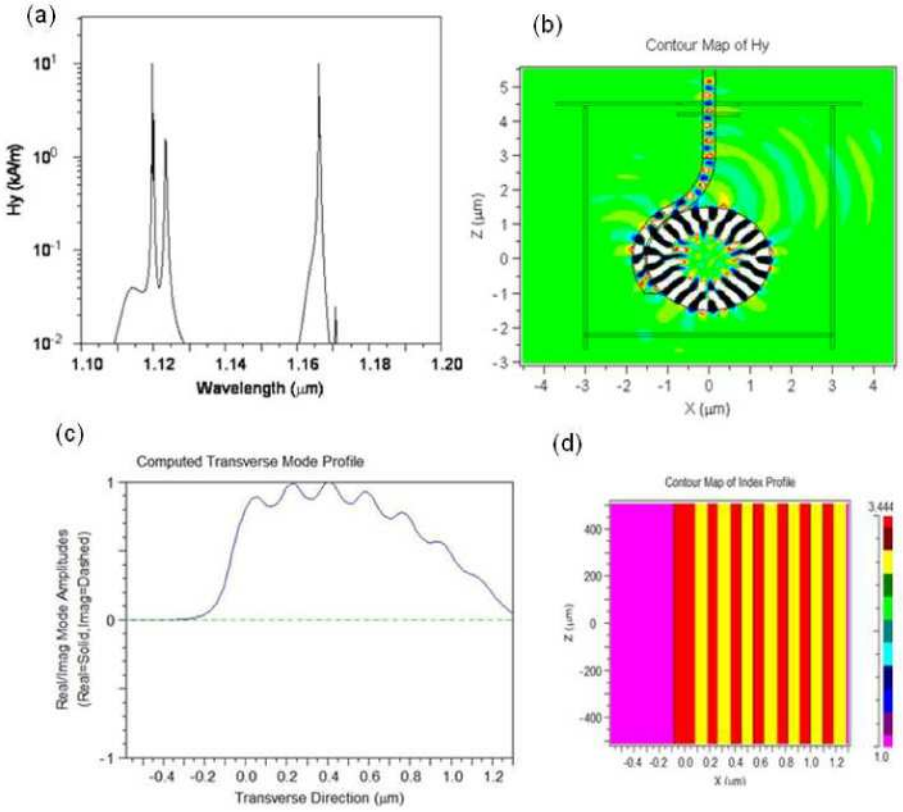

Fig. 2. (a) Magnetic field (H_y) spectrum at the centre of the waveguide and (b) Magnetic field distribution at the main resonant peak at λ=1166 nm (c) vertical distribution of the mode at λ=1166 nm (d) Refractive index profile of the epitaxially layered structure.

The vertical distribution of the main microdisk mode (H_y magnetic field) is shown in Fig. 2(c): the mode is well confined in the vertical direction but has a very asymmetric field profile. It rapidly decays to zero in the top air layer, but slowly decays to zero in the bottom Bragg stack region [this can be noted if we simultaneously observe the vertical field profile in Fig. 2(c) and the refractive index profile in Fig. 2(d)]. In fact, the electromagnetic fields extend by more than 700 nm into the Bragg layers. One way to reduce the field penetration in the Bragg stack is to use quarter wavelength layers with higher index contrast (e.g. air and GaAs).

A dipole nano-antenna can be placed directly into the single-mode waveguide. This dipole nano-antenna consists of two golden regions with a solid region between them. The metallic regions are placed at the edges of the waveguide as shown in Fig. 3(a). We assume that the width of the gap between the metallic regions is 60 nm. There are additional lateral resonant peaks due to the large reflectivity of the metallic regions in the nano-antenna. The main peak still appears at λ = 1166 nm with a reduced Q of 7000, as shown in Fig. 3(b). Another lateral

#118416 - $15.00 USD Received 12 Oct 2009; revised 23 Oct 2009; accepted 27 Oct 2009; published 30 Oct 2009

resonant peak appears at λ = 1169.4 nm with a Q of 1600. The mode with largest Q will be the fundamental mode, i.e., the first mode to reach lasing [27]. A power budget analysis indicates that, at λ=1166 nm, only 12% of the power is transmitted through the aperture and the electric field (E_x) intensity is about 1.41 MV/m (note that the electric field intensity is defined by the software and is not directly related to the laser output power). As expected, a direct coupling into the nano-antenna is not efficient and most of the power is lost to the surrounding medium and not directly coupled into the dipole antenna. There are more efficient methods to couple light into the nano-antenna as will be shown later.

3. Using tapers to couple light into the nano-antennas

Instead of direct coupling light into the nano-antenna, we can couple light by using a taper as shown in Fig. 4(a). The taper has a total length of 6 μm. We tried to avoid a very long taper but, at the same time, we tried to use a taper with sufficient length to produce a good transition between the single-mode waveguide and the aperture in the nano-antenna. The magnetic field spectrum (H_y) is shown in Fig. 4(b). The main resonant peak appears at λ=1164.8 nm with a quality factor of 12000. We can indeed couple more power into the nano-antenna with the nano-taper: the coupling efficiency increases to 30%. However, the electric field strength does not increase dramatically with the introduction of the taper: there is an increase of the amplitude of the electric field by only 30%.

A reduction in the taper length leads to a reduction in the coupling efficiency as is expected. A longer taper can couple more power into the nano-antenna, but at the expense of a larger structure. In any case, we could only couple 38% of the generated light into the single-mode waveguide without the nano-antenna, so we are close to the limit of the amount of light that could be coupled into the waveguide. The quality factor of the sidelobe at λ=1169.4 nm is reduced to 600. The introduction of the taper creates additional lateral modes in the wavelength region around the shortest wavelength edge of the material gain, indicating that this taper is reflective for these particular modes.

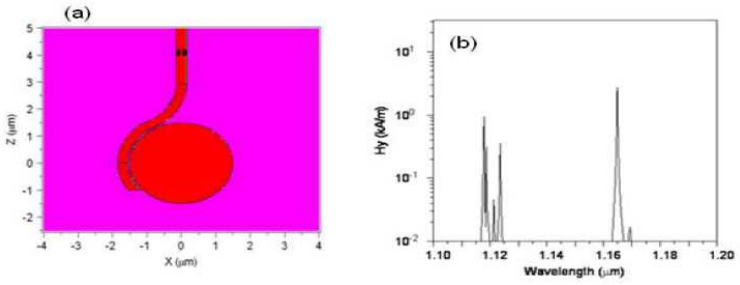

Fig. 3. (a) Direct coupling scheme from the microdisk into a nano-antenna and (b) H_y spectrum at the centre of the waveguide.

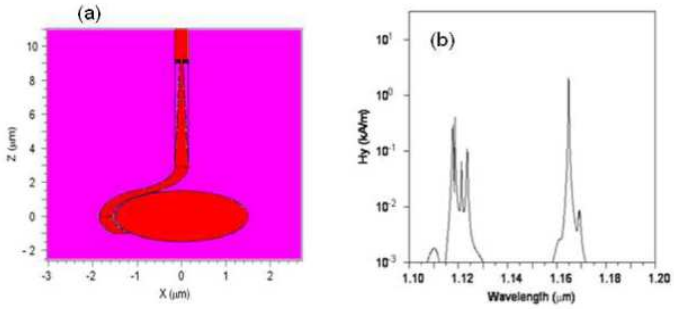

Fig. 4. (a) Microdisk coupling light to the nano-antenna via a nano-taper and (b) H_y spectrum at the centre of the waveguide.

#118416 - $15.00 USD Received 12 Oct 2009; revised 23 Oct 2009; accepted 27 Oct 2009; published 30 Oct 2009

4. Using a photonic crystal micro-cavity to couple light into nano-antennas

One way to increase the electric field inside the nano-antenna is to introduce a micro-cavity close to the antenna, as shown in Fig. 5(a). In typical laser oscillators, the circulating intensity inside the micro-cavity is considerably larger than outside it. This is because photons can bounce back and forth inside the micro-cavity and the net effect is an accumulation of photons inside the micro-cavity. This generally means that the introduction of micro-cavities to an optical system can produce regions of high intense electromagnetic fields. This effect can lead to an enhancement of the electric fields close to the nano-antenna, as will be discussed later.

However, this micro-cavity has "reflecting" components such as the air holes which can reflect light back into the microdisk resonator. The end effect is similar to what happens in optical fiber systems with very reflective fiber ends: new additional resonant modes will appear in the laser resonator. However, if these additional modes have considerably lower quality factors than the main resonant mode, we could still have a range of electrical/optical pumping power in which only one mode would be lasing before the other modes reach their threshold levels. In our case, we create a micro-cavity by adding air holes with equal diameters of 120 nm with centers positioned at distances of 200 and 350 nm "below" the "lower" edge of the nano-antenna. Hence, the cavity is created by the nano-antenna on one side and the air holes on the other side.

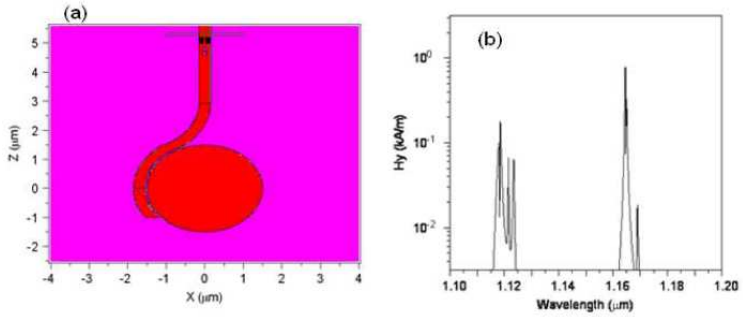

Fig. 5. (a) Micro-disk coupling light to a nano-antenna via a photonic crystal cavity and (b) H_y spectrum at the centre of the waveguide.

The magnetic field spectrum (H_y) is shown in Fig. 5(b). The microcavity formed by the nano-antenna and the air holes has a large transmission bandwidth between 1100 nm and 1400 nm. Adding more holes can increase the quality factor of the micro-cavity structure, but not much since the main escape route of photons in this micro-cavity is the nano-antenna and not the air holes.

Now, when this micro-cavity is added to the microdisk resonator, several resonant peaks appear in the gain region of the quantum dots. The main peak appears at $\lambda = 1164.5$ nm with Q of 13000. Lateral peaks appear at $\lambda = 1165$ nm with Q of 4000, $\lambda = 1169$ nm with Q of 1800 and several peaks at the shortest wavelength edge of the gain region of the quantum dots, around 1120 nm (the main peak in this region appears at 1118.6 nm with Q of 2000).

The magnetic field distribution at the main peak ($\lambda = 1164.5$ nm) is shown in Fig. 6(a). A power budget analysis indicates that about 21% of the generated power is transmitted through the nano-antenna. This amount is higher than in the case of direct coupling of light but is definitely lower than in the case where we used a nano-taper to couple light into the nano-antenna. On the other hand, the electric field has doubled with the introduction of the air holes and the creation of the micro-cavity. Electric field enhancement occurs in other devices such as vertical emitting cavity surface emitting lasers (VCSELs). Since one of the main ideas of nano-antennas is to generate high intense electric fields in small regions that could trigger surface enhanced Raman scattering (SERS) locally, the micro-cavity has further boosted the electric field in the nano-antenna and, at the same time, improved the coupling efficiency into

#118416 - $15.00 USD Received 12 Oct 2009; revised 23 Oct 2009; accepted 27 Oct 2009; published 30 Oct 2009

the nano-antenna. We can clearly observe, in Figs. 6(b) and 6(c), that the electric field is very intense in the gap between the two metallic regions of the nano-antenna.

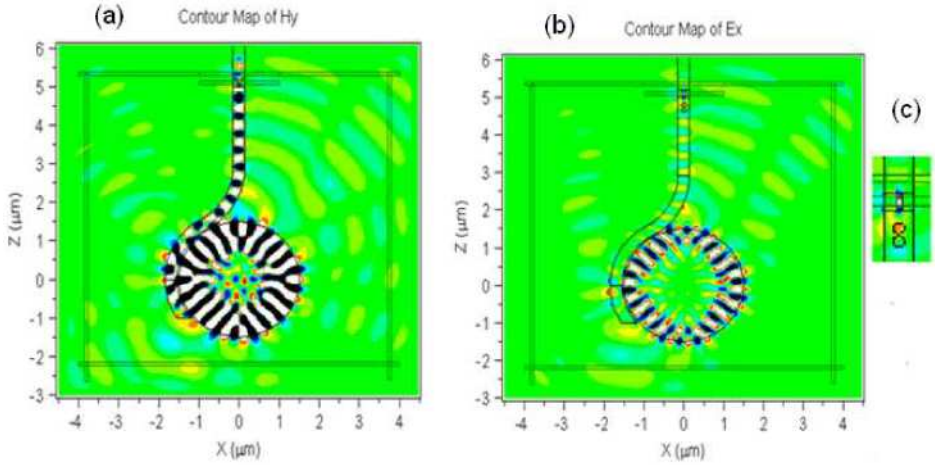

Fig. 6. Field distributions at the main peak at λ=1164.5 nm: (a) Magnetic field distribution (H_y), (b) Electric field (E_x) distribution and (c) Highlight of the electric field in the nano-antenna

A general guideline for the optimization of the photonic crystal cavity and the nano-antenna is provided below:

1. We need to minimize the reflection of the micro-cavity structure composed by the nano-antenna and air holes at the transmission peaks of the combined structure (micro-cavity structure). This means that we need to optimize the position and diameters of the air holes to maximize the transmission at the resonant peaks of the structure. As mentioned previously, the escape rate of light through the nano-antenna is generally much higher than the escape rate of light through the nano-holes, so two or three holes should be enough to boost the electric field inside the nano-antenna (more holes will not increase the Q of the micro-cavity).

2. We should try to design the micro-cavity structure to support a single longitudinal mode in the cavity. This may reduce the number of resonant peaks when we merge the microdisk resonator with this structure.

3. We need to match the transmission peak of the micro-cavity structure composed by the nano-antenna and air holes to match the main resonant peak (the peak with the highest Q in the gain bandwidth of the quantum dots). At the same time, when we merge the microdisk and the micro-cavity structure, we need to change slightly the dimensions and positions of the air holes to minimize the number of peaks in the gain region of the quantum dots. If we create additional lateral modes by merging the microdisk and the micro-cavity, we should try to make sure that they will have much lower Q when compared with the Q of the main mode or that they appear outside the gain region of the quantum dots.

6. Conclusions

In this article, we analyzed different coupling schemes to couple light from a microdisk laser into a plasmonic nano-antenna. We showed that a direct coupling into the nano-antenna isn't efficient, but if we either use a nano-taper or a low quality-factor micro-cavity we can improve the coupling efficiency into the nano-antenna. Moreover, the addition of a micro-cavity can further enhance the amplitude of the electric field inside the nano-antenna.

#118416 - $15.00 USD Received 12 Oct 2009; revised 23 Oct 2009; accepted 27 Oct 2009; published 30 Oct 2009